Bio-inspired Catalysts

International Edition: DOI: 10.1002/anie.201502364
German Edition: DOI: 10.1002/ange.201502364

Direct Comparison of the Performance of a Bio-inspired Synthetic Nickel Catalyst and a [NiFe]-Hydrogenase, Both Covalently Attached to Electrodes**

Patricia Rodriguez-Maciá, Arnab Dutta, Wolfgang Lubitz, Wendy J. Shaw, and Olaf Rüdiger**

Abstract: *The active site of hydrogenases has been a source of inspiration for the development of molecular catalysts. However, direct comparisons between molecular catalysts and enzymes have not been possible because different techniques are used to evaluate both types of catalysts, minimizing our ability to determine how far we have come in mimicking the enzymatic performance. The catalytic properties of the* $[Ni(P^{Cy}_2N^{Gly}_2)_2]^{2+}$ *complex with the [NiFe]-hydrogenase from Desulfovibrio vulgaris immobilized on a functionalized electrode were compared under identical conditions. At pH 7, the enzyme shows higher activity and lower overpotential with better stability, while at low pH, the molecular catalyst outperforms the enzyme in all respects. This is the first direct comparison of enzymes and molecular complexes, enabling a unique understanding of the benefits and detriments of both systems, and advancing our understanding of the utilization of these bio-inspired complexes in fuel cells.*

In recent years, dihydrogen has emerged as a good candidate for a sustainable carbon neutral energy economy. Energy from renewable sources can be stored in the H–H bond and employed later in fuel cells or in other chemical transformations, such as the formation of ammonia or CO_2 capture to produce hydrocarbons.[1] Platinum metal is currently used in fuel cells, but because it is rare and expensive, finding alternative efficient catalysts based on earth abundant metals for hydrogen production or uptake is an important research goal.

[*] P. Rodriguez-Maciá, Prof. W. Lubitz, Dr. O. Rüdiger
Max-Planck-Institut für Chemische Energiekonversion
Stiftstrasse 34–36, 45470 Mülheim an der Ruhr (Germany)
E-mail: olaf.ruediger@cec.mpg.de
Dr. A. Dutta, Dr. W. J. Shaw
Pacific Northwest National Laboratory
902 Battelle Blvd., Richland, WA 99354 (USA)
E-mail: wendy.shaw@pnnl.gov

[**] We would like to thank Patricia Malkowski for the purification of the *Dv*MF [NiFe]-hydrogenase and Birgit Nöring for technical assistance. We would also like to thank Adnan Sarfaz from the Max Planck Institut für Eisenforschung for the XPS measurements. P.R., W.L., and O.R. acknowledge funding from the Max Planck Society and by the Cluster of Excellence RESOLV (EXC1069) funded by the Deutsche Forschungsgemeinschaft (DFG). A.D. and W.J.S. acknowledge the Office of Science Early Career Research Program through the US Department of Energy (US DOE), Office of Science, Office of Basic Energy Sciences (BES). Pacific Northwest National Laboratory (PNNL) is operated by Battelle for the US DOE.

Supporting information for this article is available on the WWW under http://dx.doi.org/10.1002/anie.201502364.

Enzymes are used by living organisms to perform all catalytic processes in the cell. Hydrogenases are a class of metalloenzymes that catalyze the reversible oxidation of molecular hydrogen to protons and electrons.

$$H_2 \rightleftharpoons 2H^+ + 2e^- \quad (1)$$

The reactions take place at specialized Ni- and/or Fe-containing active centers that increase the acidity of H_2 and lead to heterolytic splitting of the molecule.[2] Heterolytic cleavage is accelerated by the presence of a nearby base (pendant amine for [FeFe]-hydrogenases[3] or a cysteine residue in [NiFe]-hydrogenases[4,5]). Additionally, the protein scaffold contains a series of strategically positioned iron–sulfur clusters to transfer electrons between the active site and the surface of the protein, as well as polar/acidic amino acid residues for H^+ transport.[2] This optimized assembly has enabled hydrogenases to reach turnover frequencies (TOF) as high as $20000\ s^{-1}$ at minimal overpotential (η)[6] and even outperform Pt in polymer electrolyte fuel cells.[7]

Recent work on semi-artificial maturation of hydrogenases has shown that the protein scaffold plays a crucial role in the active site efficiency.[8] Evidence of the importance of the outer coordination sphere for molecular catalysts has also been found for the $[Ni(P^R_2N^{R'}_2)_2]^{2+}$ hydrogenase mimics (P_2N_2 = 1,5-diaza-3,7-diphosphacyclooctane). These functional mimics include a pendant amine, which is found in the second coordination sphere of [FeFe]-hydrogenases, to facilitate proton transport to and from the active site.[9] The catalytic performance of these Ni complexes was improved by the inclusion of an enzyme-inspired peptide or amino acid based outer coordination sphere.[10] The incorporation of a single amino acid on the pendant amine groups of the $[Ni(P^{Cy}_2N^{R'}_2)_2]^{2+}$ complex created a minimal H^+ transport pathway, resulting in water solubility, improved rates, and reduced overpotential.[11]

Herein, we provide a direct comparison of the function of the $[Ni(P^{Cy}_2N^{R'}_2)_2]^{2+}$ complexes to enzymatic function. The carboxylic acid groups of the catalyst containing four glycines (Gly), $[Ni(P^{Cy}_2N^{Gly}_2)_2]^{2+}$,[11c] are used to covalently attach the complex to an amine functionalized carbon electrode (Scheme 1 and Supporting Information), using the same method employed to attach the *Desulfovibrio vulgaris* Miyazaki F (*Dv*MF) [NiFe]-hydrogenase to the electrode.[12] This immobilization was performed in water, and provides a simple and enzyme-compatible alternative to the immobilization recently reported for similar catalysts using organic solvents.[13] This allowed us to compare, for the first time, the performance of the catalyst and enzyme under identical conditions.

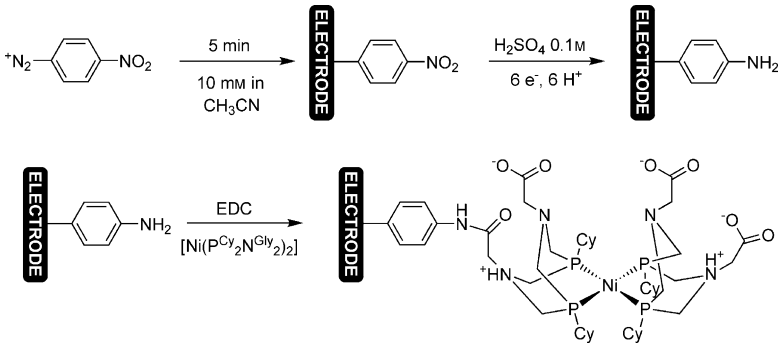

Scheme 1. Idealized representation of the covalent immobilization of the $[Ni(P^{Cy}_2N^{Gly}_2)_2]^{2+}$ catalyst on a carbon electrode. EDC = 1-ethyl-3-(3-dimethylaminopropyl)carbodiimide. Additional binding options are shown in the Supporting Information, Scheme S1.

Upon immobilization of the $[Ni(P^{Cy}_2N^{Gly}_2)_2]^{2+}$ on the electrode, the measured cyclic voltammetry (CV) under N_2 in Figure 1 (for details, see the Supporting Information, Figure S1 and Experimental Section) shows a reversible wave at −263 mV (at pH 7.0) with a full-width at half-maximum very close to 91 mV.[14] These signals were identified in solution as two overlapping one-electron processes resulting from the reduction of Ni^{II} to Ni^0.[11c] The intensity of these peaks varies linearly with the scan rate, as expected for a surface immobilized species (Supporting Information, Figure S2).[14] Integration of the charge under these peaks provides a direct measure of the surface concentration of the immobilized catalyst.

Immobilization from solutions of 1 mM or higher yielded a catalyst surface coverage of 21 ± 7 pmol cm^{-2} (*based on five trials*), the same order of magnitude as reported for similar complexes immobilized on surfaces.[13] The turnover frequency (TOF) at pH 7.0 is 10 s^{-1}, increasing under more acidic conditions, as shown in Table 1, and is consistent with the catalyst performance in solution, though with slightly higher rates at low pH. TOFs were determined from the i_{cat} and the measured coverage for each individual electrode using Equation (2), assuming a first-order dependence on the

$$\mathrm{TOF} = \frac{i^{cat}}{nFA\Gamma} \qquad (2)$$

catalyst surface coverage (Γ), where n is the number of electrons per turnover (2), F is the Faraday constant, and A is the area of the electrode (0.196 cm^2). The measured catalytic current was independent of the rotation rate (at rotation rates beyond 1500 rpm; Supporting Information, Figure S3), indicating that catalysis is not limited by substrate diffusion to the electrode.

Unfortunately, TOF values for the hydrogenase-modified electrode could not be quantified. These are ideally quantitated using the signals arising from the reduction of the [FeS] clusters, but in our case, non-catalytic signals arising from the [FeS] clusters could not be recorded, indicating a low hydrogenase coverage. An enzyme coverage of 0.6 pmol cm^{-2} on the electrodes could be estimated from its activity in solution (729 s^{-1} at pH 7.6, 25 °C and in the presence of benzyl viologen as an electron acceptor), using Equation (2) and the H_2 oxidation catalytic current measured in the CV of the hydrogenase-modified electrode. Alternatively, an exception-

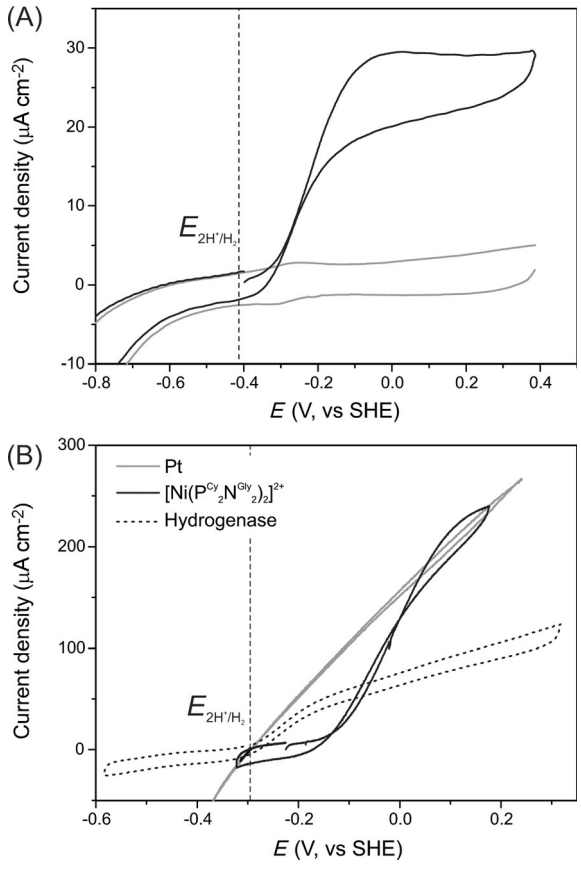

Figure 1. A) Cyclic voltammograms (CV) of an HOPG electrode covalently modified with $[Ni(P^{Cy}_2N^{Gly}_2)_2]^{2+}$, under N_2 (gray trace) and under 1 bar H_2 (black trace) recorded at 20 mV s^{-1}, pH 7.0 $HClO_4$ 0.1 M and 2000 rpm rotation rate. B) CV measurements of a Pt disc electrode (gray trace), a *Dv*MF [NiFe] hydrogenase modified electrode (dashed black trace), and a $[Ni(P^{Cy}_2N^{Gly}_2)_2]^{2+}$ (solid black trace) modified electrode, comparing the onset potentials for each catalyst. Conditions: 20 mV s^{-1}, pH 5.0, 0.1 M Na_2SO_4/0.1 M MES/HEPES, 1 bar H_2, 25 °C and 2000 rpm rotation rate. The vertical dashed lines represent the equilibrium potential for 2 H^+/H_2 couple.

Table 1: Comparison of overpotential (η) and TOF values obtained for $[Ni(P^{Cy}_2N^{Gly}_2)_2]^{2+}$ covalently immobilized on the electrode and in solution at 25 °C.[11c]

pH	η covalent[a] [mV]	η solution[b] [mV]	TOF covalent[a] [s^{-1}]	TOF solution[b] [s^{-1}]
2	174	160	66	21
3	225	n.d.	26	n.d.
3.5	n.d.	240	n.d.	3
4	217	n.d.	10	n.d.
5	207	265	4	5
6	197	270	4	6
7	231	285	10	8
8	237	325	14	7

[a] This work. [b] Ref.[11c]. n.d. = not determined.

ally high coverage of 1 to 3 pmol cm^{-2} has been reported for similar hydrogenases.[15] Even if the higher coverage was assumed, the rate of *Dv*MF is still more than one order of magnitude faster than the Ni complex at pH 7.0 under identical conditions. As is usually reported for hydrogenases,[16] the catalytic current for H_2 oxidation drops at lower pH values, and when the pH is below 4.0, the activity is irreversibly lost for the enzyme as a result of protein denaturation.

Despite the electrode-immobilized $[Ni(P^{Cy}_2N^{Gly}_2)_2]^{2+}$ having a lower TOF at neutral pH, it exhibited higher catalytic currents than for the hydrogenase-modified electrode (Figure 1B). This observation can be explained based on the size of both catalysts (with a molecular mass of 90 kDa and a diameter of 45 Å for hydrogenase[5] and about 1 kDa for $[Ni(P^{Cy}_2N^{Gly}_2)_2]^{2+}$), which yields a circa 30 times higher coverage for the synthetic catalyst, a decisive advantage for the molecular complex in practical applications. Achieving this level of coverage for hydrogenase would require a three-dimensional polymeric matrix.

To obtain a direct comparison of the overpotential of the catalyst with that of hydrogenase, the CV of the $[Ni(P^{Cy}_2N^{Gly}_2)_2]^{2+}$ modified electrode was compared with the hydrogenase-modified electrode and a Pt electrode, as shown in Figure 1B. Pt, a very efficient reversible catalyst,[17] is used here as a reference.[17] Hydrogenase begins to oxidize H_2 at almost no overpotential at pH 5.0, while the onset potential for the $[Ni(P^{Cy}_2N^{Gly}_2)_2]^{2+}$ starts 146 mV more positive under the same conditions. In the Supporting Information, Figure S4, we show the CVs recorded at different pH values (from pH 7.0 to 2.1) under 1 bar of H_2 at 25 °C. For the enzyme, the onset potential shifts 60 mV per pH unit as expected from the Nernst equation.[18] The overpotential (η) for the immobilized $[Ni(P^{Cy}_2N^{Gly}_2)_2]^{2+}$ catalyst exhibited less dependence upon the pH (pH range = 2.1–8.0) than the same complex in solution, which was attributed to improved electron transfer between the catalyst and electrode after immobilization (Table 1). The overpotential was determined using the same method described by Appel et al.[19]

H_2 production by the [NiFe]-hydrogenase of *Dv*MF is strongly inhibited by the presence of H_2 in solution.[20] Diluting $[H_2]$ to 50% with N_2 results in a reduction current observed at the expected thermodynamic potential for H^+ reduction, with the CV sharply crossing the zero current line (Figure 2A; collected at 50 °C to increase the rate of H_2 production for the Ni complex, but also observed at 25 °C). The $[Ni(P^{Cy}_2N^{Gly}_2)_2]^{2+}$ catalyst also shows a reduction current at low pH values and 50 °C (Figure 2B; Supporting Information, Figure S6), operating at the equilibrium potential for both H_2 oxidation and production, a behavior that was not observed at room temperature (Figure 1B). The complex also operates reversibly at elevated temperatures in solution, further suggesting that immobilization has not altered the catalytic performance.[11b] A plateau current in the H_2 production was not reached, even extending the measurement to lower potentials (Supporting Information, Figure S6). This could be consistent with two different (and slightly overlapping) processes for H_2 production, as observed in solution, one of which is reversible, and the second which operates at a higher overpotential (starting around −250 mV at pH 2; Figure 2) and is not part of the reversible process.[11b] The TOF and η for H_2 production by the Ni catalyst were not determined owing to the complex nature of these waves.

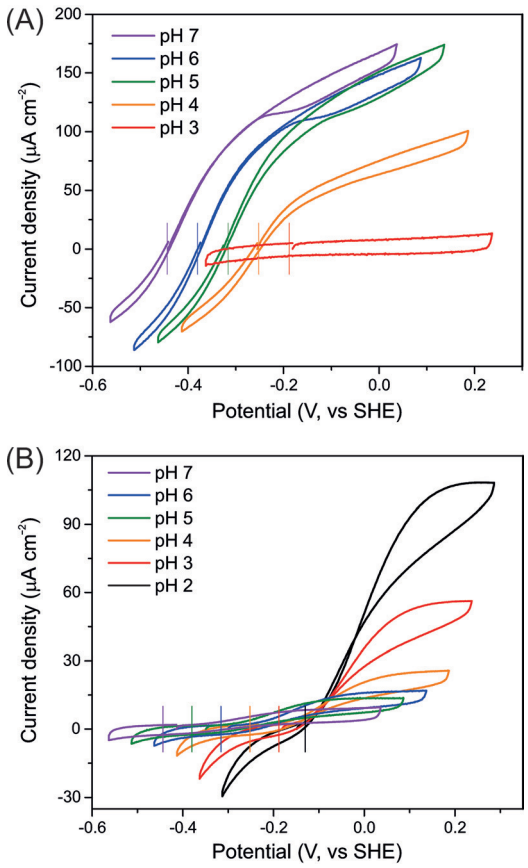

Figure 2. Cyclic voltammograms (CV) of an HOPG electrode covalently modified with *Dv*MF [NiFe] hydrogenase (A) or $[Ni(P^{Cy}_2N^{Gly}_2)_2]^{2+}$ (B), recorded at several pH values, 20 mV s^{-1}, 50 °C, 1 bar 50% H_2 in N_2 with a total gas flow of 1500 mL min^{-1} and a rotation rate of 2000 rpm. The vertical lines indicate the thermodynamic redox potential for the H^+ reduction reaction at each pH value.

One of the aspects which can be examined in detail on the surface-confined catalyst is its long term stability. When measured in solution, the bulk of the solution acts as a reservoir of "fresh" catalyst, masking catalyst decomposition processes. This is not the case when there is only a small amount of catalyst confined on the surface of the electrode, as in the current experiments. While the immobilized hydrogenase is very stable, based upon the current for H_2 oxidation in a chronoamperometric experiment, with almost no observed drop in current over three days, the catalytic currents for the immobilized catalyst dropped to 25% in about six hours (Figure 3A). To examine the stability of the immobilized Ni-complex in more detail, 10 consecutive CVs were measured monitoring the Ni-redox wave under non-catalytic conditions. The area corresponding to the Ni oxidation/reduction peaks stayed constant over the experiment (less than 2% anodic peak area lost; Supporting Information, Figure S7). On the other hand, when several CVs under H_2 are measured, the catalytic oxidation and

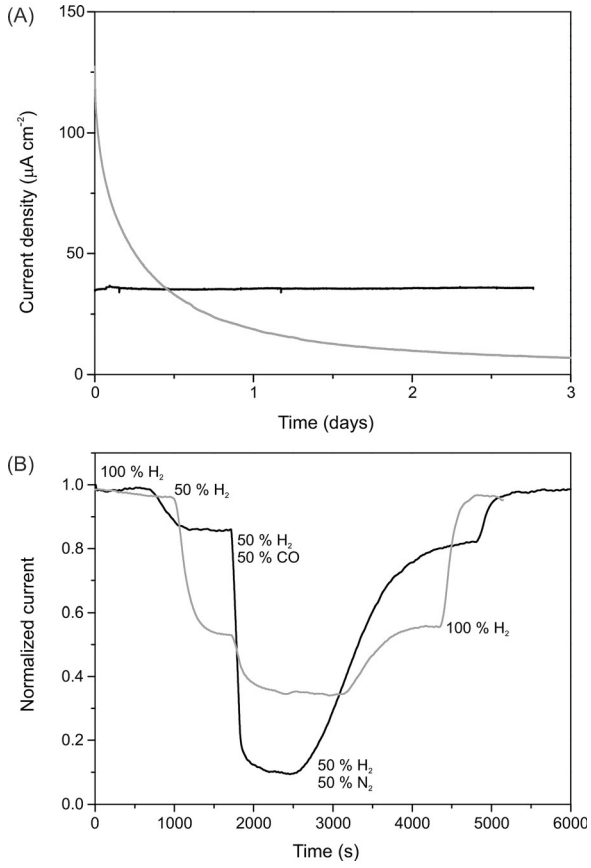

Figure 3. Chronoamperometric measurements on HOPG electrodes covalently modified with $[Ni(P^{Cy}_2N^{Gly}_2)_2]^{2+}$ (gray trace, E = −0 V vs. SHE) and *Dv*MF [NiFe]-hydrogenase (black, E = −0.21 V vs. SHE) (A) to study the stability of the catalyst for H_2 oxidation catalysis on the electrode. B) To study H_2 oxidation inhibition by CO. Gas composition changes are indicated on the figure, the total gas flow though the cell was 1500 mL min^{-1}. All data collected at 25 °C, 2000 rpm rotation rate, and conditions which were found to be optimal for the respective catalyst, that is, pH 2.1, $HClO_4$ 0.1 M for the Ni catalyst and pH 7.0, 0.1 M Na_2SO_4/0.1 M MES/HEPES for the hydrogenase electrode.

reduction currents decrease rapidly upon successive measurements, while the H^+ reduction current at low potentials remains constant (Supporting Information, Figure S8). Decomposition was slower when measured at 25 °C, pH 2.1, and 25 % H_2 (Supporting Information, Figure S8). These data suggest that the catalyst responsible for H_2 oxidation suffers irreversible degradation to form another species that is still able to reduce H^+ at higher overpotential.

Decomposition is further supported by X-ray photoelectron spectroscopic (XPS) studies, where a shoulder on the Ni $2p_{3/2}$ region characteristic of Ni^0 species (851.2 eV)[21] was found on the spectra of an HOPG "edge" plate measured on an electrode that had been monitored for H_2 oxidation until the current was completely lost. This shoulder was not present in the spectra recorded for the immobilized catalyst before recording any catalytic current (Supporting Information, Figure S9 and Table S2). To confirm that the loss in signal is not due to desorption, the stability of the covalent bond between the catalyst and the electrode was studied using surface-enhanced IR absorption spectroscopy (SEIRAS). Using a gold surface modified with a 4-aminothiophenol (4-ATP) self-assembled monolayer (SAM),[22] it was possible to monitor the amide band formation and stability during a chronoamperometric measurement. The recorded spectra (Supporting Information, Figure S10) show that the intensity of the band assigned to the amide CO group does not change over the chronoamperometric measurement, while the catalytic H_2 oxidation current significantly decreases after 2 h. Another possibility that cannot be excluded based on these data is that the immobilization method imposes a rigid conformation onto $[Ni(P^{Cy}_2N^{Gly}_2)_2]^{2+}$,[23] such as multiple carboxylates binding to the electrode (Supporting Information, Scheme S1). This may enhance its degradation over time. Experiments are ongoing to provide insight into the degradation mechanism.

The stability of the catalysts in the presence of impurities in the fuel feed is also an important consideration for practical implementation. Standard hydrogenases such as *Dv*MF are strongly inhibited by CO, which blocks the open coordination site, binding to the Ni in the Ni–C or Ni–SI_a states.[2] But unlike Pt catalysts, which require harsh oxidative treatment to remove the adsorbed CO,[24] [NiFe]-hydrogenases can be completely reactivated upon displacement of CO (Figure 3B) and the so-called oxygen tolerant hydrogenases retain their activity in the presence of CO.[25] We found that CO inhibits the H_2 oxidation activity of $[Ni(P^{Cy}_2N^{Gly}_2)_2]^{2+}$, but to a lesser extent than for *Dv*MF. This inhibition is also completely reversible, as observed in solution[11a,26] or on immobilized carbon nanotubes.[27] This presents an additional practical advantage over precious metal catalysts, since the Ni catalyst could operate in a fuel cell using the common lower purity H_2 coming from steam reforming.

Oxygen is another well-known inhibitor of hydrogenases. The way that *Dv*MF is rapidly inactivated by O_2 is shown in the Supporting Information, Figure S11. This inactivation is partially reversible and leads to the formation of several inactive states which can be recovered upon reductive reactivation.[2] On the other hand, $[Ni(P^{Cy}_2N^{Gly}_2)_2]^{2+}$ reacts slower than the hydrogenase with O_2 but its inactivation is completely irreversible, which is in agreement with the oxidation of the diphosphine ligands in air, resulting in disassociation.[11a,28]

In summary, here we report the first direct electrochemical comparison between a bio-inspired synthetic catalyst and a [NiFe]-hydrogenase, which are immobilized similarly on electrodes using simple chemistry. The H_2 oxidation overpotential of the Ni catalyst is unambiguously measured and directly compared with the hydrogenase, both of which operate at the equilibrium potential under their optimal conditions (low pH/elevated temperature for the Ni complex and neutral pH for hydrogenase). The overall catalytic performance comparison with hydrogenase highlights the remarkable efficiency of these Ni catalysts, outperforming the [NiFe]-hydrogenase from *Dv*MF at low pH values and in the presence of substantial amounts of CO. These characteristics indicate that the Ni catalysts are ideal candidates for proton-exchange membrane (PEM) fuel cells, where low pH and high temperatures are present, and inexpensive low purity H_2

could be used as a fuel. The long term stability of the catalyst and its O_2 sensitivity remains to be solved.

Keywords: enzyme catalysis · hydrogen oxidation · hydrogenases · molecular catalysis · surface-immobilized catalysis

How to cite: *Angew. Chem. Int. Ed.* **2015**, *54*, 12303–12307
Angew. Chem. **2015**, *127*, 12478–12482

[1] a) N. S. Lewis, D. G. Nocera, *Proc. Natl. Acad. Sci. USA* **2006**, *103*, 15729–15735; b) J. J. Concepcion, R. L. House, J. M. Papanikolas, T. J. Meyer, *Proc. Natl. Acad. Sci. USA* **2012**, *109*, 15560–15564.
[2] W. Lubitz, H. Ogata, O. Ruediger, E. Reijerse, *Chem. Rev.* **2014**, *114*, 4081–4148.
[3] A. Silakov, B. Wenk, E. Reijerse, W. Lubitz, *Phys. Chem. Chem. Phys.* **2009**, *11*, 6592–6599.
[4] K. Weber, T. Krämer, H. S. Shafaat, T. Weyhermüller, E. Bill, M. van Gastel, F. Neese, W. Lubitz, *J. Am. Chem. Soc.* **2012**, *134*, 20745–20755.
[5] H. Ogata, K. Nishikawa, W. Lubitz, *Nature* **2015**, *520*, 571–574.
[6] C. Madden, M. D. Vaughn, I. Díez-Pérez, K. A. Brown, P. W. King, D. Gust, A. L. Moore, T. A. Moore, *J. Am. Chem. Soc.* **2012**, *134*, 1577–1582.
[7] T. Matsumoto, S. Eguchi, H. Nakai, T. Hibino, K.-S. Yoon, S. Ogo, *Angew. Chem. Int. Ed.* **2014**, *53*, 8895–8898; *Angew. Chem.* **2014**, *126*, 9041–9044.
[8] a) G. Berggren, T. Simmons, A. Adamska, C. Lambertz, J. Esselborn, M. Atta, S. Gambarelli, J. M. Mouesca, E. J. Reijerse, W. Lubitz, T. Happe, V. Artero, M. Fontecave, *Nature* **2013**, *499*, 66–69; b) J. Esselborn, C. Lambertz, A. Adamska, T. Simmons, G. Berggren, J. Noth, J. F. Siebel, A. Hemschemeier, V. Artero, E. J. Reijerse, M. Fontecave, W. Lubitz, T. Happe, *Nat. Chem. Biol.* **2013**, *9*, 607–609.
[9] D. L. DuBois, *Inorg. Chem.* **2014**, *53*, 3935–3960.
[10] B. Ginovska-Pangovska, A. Dutta, M. L. Reback, J. C. Linehan, W. J. Shaw, *Acc. Chem. Res.* **2014**, *47*, 2621–2630.
[11] a) A. Dutta, J. A. S. Roberts, W. J. Shaw, *Angew. Chem. Int. Ed.* **2014**, *53*, 6487–6491; *Angew. Chem.* **2014**, *126*, 6605–6609; b) A. Dutta, D. L. DuBois, J. A. S. Roberts, W. J. Shaw, *Proc. Natl. Acad. Sci. USA* **2014**, *111*, 16286–16291; c) A. Dutta, S. Lense, J. Hou, M. H. Engelhard, J. A. S. Roberts, W. J. Shaw, *J. Am. Chem. Soc.* **2013**, *135*, 18490–18496.
[12] O. Rüdiger, J. M. Abad, E. C. Hatchikian, V. M. Fernández, A. L. de Lacey, *J. Am. Chem. Soc.* **2005**, *127*, 16008–16009.
[13] A. K. Das, M. H. Engelhard, R. M. Bullock, J. A. S. Roberts, *Inorg. Chem.* **2014**, *53*, 6875–6885.
[14] E. Laviron, *J. Electroanal. Chem.* **1979**, *101*, 19–28.
[15] a) H. R. Pershad, J. L. C. Duff, H. A. Heering, E. C. Duin, S. P. J. Albracht, F. A. Armstrong, *Biochemistry* **1999**, *38*, 8992–8999; b) A. Parkin, G. Goldet, C. Cavazza, J. C. Fontecilla-Camps, F. A. Armstrong, *J. Am. Chem. Soc.* **2008**, *130*, 13410–13416.
[16] K. A. Vincent, A. Parkin, F. A. Armstrong, *Chem. Rev.* **2007**, *107*, 4366–4413.
[17] A. K. Jones, E. Sillery, S. P. J. Albracht, F. A. Armstrong, *Chem. Commun.* **2002**, 866–867.
[18] A. J. Bard, L. R. Faulkner, *Electrochemical Methods: Fundamentals and Applications*, 2nd ed. ed., Wiley, New York, **2001**.
[19] A. M. Appel, M. L. Helm, *ACS Catal.* **2014**, *4*, 630–633.
[20] H. S. Shafaat, O. Rüdiger, H. Ogata, W. Lubitz, *Biochim. Biophys. Acta Bioenerg.* **2013**, *1827*, 986–1002.
[21] A. P. Grosvenor, M. C. Biesinger, R. S. Smart, N. S. McIntyre, *Surf. Sci.* **2006**, *600*, 1771–1779.
[22] O. Gutiérrez-Sanz, M. Marques, I. A. C. Pereira, A. L. de Lacey, W. Lubitz, O. Rüdiger, *J. Phys. Chem. Lett.* **2013**, *4*, 2794–2798.
[23] D. H. Pool, D. L. DuBois, *J. Organomet. Chem.* **2009**, *694*, 2858–2865.
[24] J. J. Baschuk, X. G. Li, *Int. J. Energy Res.* **2001**, *25*, 695–713.
[25] K. A. Vincent, J. A. Cracknell, O. Lenz, I. Zebger, B. Friedrich, F. A. Armstrong, *Proc. Natl. Acad. Sci. USA* **2005**, *102*, 16951–16954.
[26] a) A. D. Wilson, K. Fraze, B. Twamley, S. M. Miller, D. L. DuBois, M. Rakowski DuBois, *J. Am. Chem. Soc.* **2008**, *130*, 1061–1068; b) D. W. Wakerley, M. A. Gross, E. Reisner, *Chem. Commun.* **2014**, *50*, 15995–15998.
[27] P. D. Tran, A. Le Goff, J. Heidkamp, B. Jousselme, N. Guillet, S. Palacin, H. Dau, M. Fontecave, V. Artero, *Angew. Chem. Int. Ed.* **2011**, *50*, 1371–1374; *Angew. Chem.* **2011**, *123*, 1407–1410.
[28] J. Y. Yang, R. M. Bullock, W. G. Dougherty, W. S. Kassel, B. Twamley, D. L. DuBois, M. R. DuBois, *Dalton Trans.* **2010**, *39*, 3001–3010.

Received: March 13, 2015
Published online: July 3, 2015

